Critical Experimental Comparison between Five Techniques for the Determination of Interfacial Tension in Polymer Blends: Model System of Polystyrene/Polyamide-6

Peixiang Xing, M. Bousmina,* and D. Rodrigue

Department of Chemical Engineering, CERSIM, Laval University, Sainte-Foy, Quebec G1K 7P4, Canada

M. R. Kamal

Department of Chemical Engineering, McGill University, Montreal, Quebec H3A 2A7, Canada

Received March 27, 2000; Revised Manuscript Received June 13, 2000

ABSTRACT: A critical review and experimental comparison between different techniques for the determination of interfacial tension are presented for a model polymer pair. Five experimental methods were applied to measure the interfacial tension for the model pair of polystyrene (PS) and polyamide-6 (PA-6) at the same temperature. The techniques include three dynamic methods (the breaking thread method, the imbedded fiber retraction method, and the retraction of deformed drop method), one equilibrium method (the pendant drop method), and a rheological method based on linear viscoelastic measurements. The advantages, the limitations, and the difficulties of each technique are discussed and compared.

Introduction

Interfacial tension plays a predominant role in multiphase systems, such as polymer blends and alloys. The properties of polymer blends are directly related to the properties of the components, to their morphology (distribution and dispersion of the phases), and to the properties of the interface/interphase. Interfacial tension is one of the essential parameters in characterizing and quantifying the interactions at such interface/interphase.

Various techniques[1,2] are available for the determination of the interfacial tension. The general principle of these techniques is based on a balance between a driving force (Brownian forces, gravitational and inertia forces, or viscous forces) and a resistance due to the interfacial force that tends to minimize the contact area between the phases.

The various techniques can generally be divided into two categories: equilibrium and transient methods. The equilibrium methods include the "pendant drop",[3−5] the "sessile drop",[6] and the "spinning drop" methods.[7,8] The dynamic methods include the "breaking thread",[9−11] the "retraction of deformed drop",[12] the "imbedded fiber retraction",[13−15] and the "imbedded disk retraction" methods.[16]

In equilibrium methods, the interfacial tension is determined in the final state where the system has reached equilibrium, while in the dynamic methods, the liquid−liquid interfacial shape changes as a function of time, and the interfacial tension, γ_{12}, is determined from the time evolution of the interfacial profile using a given model for the thread distortion, the fiber retraction, or the return of a distorted fluid particle toward its equilibrium shape.

Another category of methods is the rheological method that is based on oscillatory shear measurements at small amplitude of deformation.

* To whom all correspondence should be addressed.

In this paper, we propose to offer the first critical experimental comparison between five methods. The methods used in this work are (i) breaking thread, (ii) imbedded fiber retraction, (iii) retraction of deformed drop, (iv) pendant drop, and (v) a rheological method. All the techniques were performed at the same temperature for a given model polymer pair: polystyrene (PS) and polyamide (PA-6). For each method, the principle, the basic equations, and the experimental results are critically exposed and discussed in terms of advantages, limitations, and the error sources. The application of these techniques to systems with compatibilizers is discarded here because of the complexity of the systems and the difficulty of a rigorous interpretation of the results due to the difficulty of a definite identification of the location of the compatibilizer. We should stress however that only equilibrium methods can be rigorously used in this case due to the long time required by the copolymer to diffuse and to ensure a complete interfacial segregation. This however will depend on the nature of the copolymer, on its structure, and on its molecular weight and molecular weight distribution.

Materials

The different experiments were conducted on the PS/PA-6 system. The PS, used in this work as matrix, was obtained from NOVA Chemicals (Calgary, Canada). The PA-6 was obtained from BASF (Germany). The transition temperatures (glass transition, T_g, and melting transition, T_m) and number-average molecular weight, M_n, as measured by differential scanning calorimetry (DSC) and gel permeation chromatography (GPC), respectively, are reported in Table 1. The zero shear viscosities, η_0, of the samples were measured by small-amplitude oscillatory shear measurements at 230 °C using the Bohlin CVO constant stress rheometer. The data are also reported in Table 1.

Experimental Section

Since all the experiments were performed at 230 °C, eventual thermal degradation may occur at this temperature.

10.1021/ma000537x CCC: $19.00
Published on Web 09/19/2000

Table 1. General Characteristics of the Materials

acronym	polymer	trade name	T_m (°C)	T_g (°C)	M_n	η_0 (Pa·s, 230 °C)	supplier
PS	polystyrene	PS 101-300		100	2.0×10^5	2500	NOVA
PA-6	polyamide-6	Ultramid B4	218	48	3.3×10^4	2700	BASF

To verify the thermal stability of the polymers (PS and PA-6), thermogravimetric analyses (TGA) were performed under a nitrogen atmosphere at 230 °C, using a METTLER TG50 system. The results indicated that, within a period of 17 h, no appreciable weight loss was recorded (1.1% loss for PS and 1.5% loss for PA-6). To prevent thermal degradation, the pendant drop experiment was conducted under argon gas, and all other experiments were conducted under a continuous purge of nitrogen.

Breaking Thread Methods (BTM). The technique consists of heating a thread of a given polymer sandwiched between two films of another polymer and recording the disturbances generated on the surface of the thread that breaks up to spatially aligned and spaced spheres after passing through a periodic peanutlike shape. From the viscosity ratio and the dimensions of the disturbances, one can determine the interfacial tension.

The PA-6 threads were drawn from molten pellets of PA-6 with diameters ranging from 20 to 60 μm. Before each test, the fibers were annealed in a vacuum oven for 24 h at 90 °C. (The effect of annealing is discussed in the Results section.) Two compression molded PS films with thickness of about 0.5 mm were dried in a vacuum oven for about 24 h at 70 °C before each test. The thread of PA-6, about 18 mm in length ($L/D \approx 300$), was placed between the two PS films (12 × 12 mm), and the total sandwich sample was put between a glass slide and a coverslip. Then, it was heated to a temperature of 230 °C in a HS400 hot stage equipped with a RTC1 (Instec, Inc.) temperature controller placed directly under a microscope for visual observations. The direct observation of the evolution of the thread shape was made through a CCD camera mounted on the optical Axioskop (ZEISS) microscope. The whole process was filmed and stored on high-quality professional videotape equipped with an internal chronometer. This gives the flexibility of analyzing afterward the images in the desired sequences. Visilog 4.0 (Noesis Vision Inc.) computer software was used to acquire the digitized images and to make quantitative image analysis.

Imbedded Fiber Retraction Method (IFRM). The technique is similar to the BTM, except that here the fiber is short to prevent the fiber fragmentation process. In our experiments, the fiber length was taken in the interval 0.7−1.2 mm. Under this condition, the fiber retracts to a spherical shape and the interfacial tension is determined from the viscosities of the components, the initial fiber diameter, the radius of the final drop, and the effective diameter of the fiber during retraction.

The sandwiched sample was heated at 230 °C, and the experiment was started after 5 min required for thermal equilibrium, smoothing of the fiber surface, and better immersion of PA-6 fiber into PS. The retraction of the fiber into the spherical shape was then recorded and analyzed by the same tools as those used for the breaking thread analysis.

Retraction of Deformed Drop Method (DDRM). The technique consists of deforming a given spherical drop and then recording, as a function of time, the relaxation and the return of the generated ellipsoid of revolution to the equilibrium spherical shape. The interfacial tension is then determined from the viscosities of the components and the dimensions of shape recovery of the drop. To obtain a spherical drop with well-defined contours, one can put directly a fine powder between the two films of the other polymer or alternatively use the drops generated during the breaking thread method or the drop formed after fiber retraction. If the breaking thread method is chosen to generate the drop, care has to be taken to select an isolated drop such that hydrodynamic interactions with the neighboring drops can be neglected. In our work, the drop was obtained by the fiber retraction technique. The sandwich sample was placed between the glass slides separated by a metallic guide to maintain a constant thickness. The upper plate was then manually and smoothly moved parallel to the lower plate. Although we have no accurate estimation of the shear rate in such manual manipulation, care was taken to slowly slide the upper plate to generate slow and low amplitude of deformation. The variation of the ellipsoid profile was recorded and analyzed in the same way as for the IFRM.

Pendant Drop Method (PDM). The technique consists of immersing a drop of a molten polymer into the bulk of another molten polymer. The interfacial tension is then determined from the equilibrium drop profile and from the difference in densities between the two molten polymers.

The apparatus used for the pendant drop method has been described in detail by Demarquette and Kamal.[4] Briefly, the device consists of an isolated and temperature-controlled quartz cell chamber filled with the molten polymer matrix (in our case PS). The threads of PA-6, 1.8 mm in diameter, for the pendant drop test were formed by extrusion in a capillary rheometer and subsequently placed and melted in a syringe. The heated syringe, with the PA-6, is inserted in the molten matrix in the cell. Then, a drop of the high-density polymer (PA-6), suspended from the tip of the syringe, was immersed in the cell, which had a transparent window for visualization.

The variation of the shape of the drop in time was recorded using a CCD video color camera. The profile of the drop was then evaluated by digital image analysis using the procedure described in Demarquette and Kamal.[4] The technique allows an on-line computation and quick estimation of the transient interfacial tension.[4,5,17]

Generally, the volume of the drop should be in a suitable range. If the drop of the highest density polymer is extruded into the melt of the second polymer PS with a volume smaller than the lower critical volume, the drop will become smaller and retracts back into the syringe, disappearing completely. If the volume of the drop is larger than the higher critical volume, it will neck and detach ("necking" phenomenon).[4] In the above two cases, it is not possible to obtain a stable drop and to reach the equilibrium drop profile. To avoid the capillary effect, a small ring (Rulon) is installed behind the tip of the plunger to seal the syringe capillary tube after the high-density polymer is extruded to form a drop.

In the experiments, both samples should be clear of impurities and dried to remove moisture, which can produce bubbles. After placing the compression molded PS in the quartz cell, the syringe which contains a tightly fit thread of PA-6 with a suitable diameter was inserted into the PS melt quickly. After the thread in the syringe melted, it was extruded slowly from the syringe. The volume of the extruded drop is manipulated by adjusting the initial length as observed on the computer monitor. Corrections to the observed dimensions of PA-6 in the PS melt must be made, because the refractive indices of the polymers and the glass window can cause differences between the real dimensions and those of the acquired image.

Rheological Method (RM). The rheological method consists of measuring, under small amplitude of deformation, the dynamic moduli, G' and G'' of the blend and the components. The interfacial tension is then determined from the dynamic moduli and from the particle size of the dispersed phase, as determined by electron microscopy analysis.

The dynamic viscoelastic measurements were carried out using a Bohlin-CVO stress rheometer with parallel plate geometry and a gap of 1.2 mm. The polymer blends of PS/PA-6 (90/10 and 80/20) were first prepared by melt blending at 230 °C during 12 min in a Haake batch mixer. From these blends, samples for rheological measurements with 25 mm diameter and 1.5 mm thickness were made by compression molding at 230 °C.

Before use, the samples were dried in a vacuum oven at 80 °C for 24 h. The measurements were performed under a

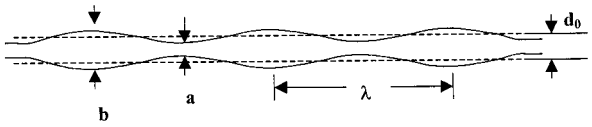

Figure 1. Schematic representation of the sinusoidal distortions of a liquid cylinder. d_0 is the initial diameter of the fiber; b and a are the maximum and minimum diameters of the fiber during distortion.

nitrogen atmosphere, employing a frequency sweep from 10^{-3} to 20 Hz. The stress was automatically adjusted to keep the measurements in the linear regime. The average particle size was determined by morphological analysis of PS/PA-6 (90/10, 80/20) blends using a JEOL-840A scanning electron microscope. The observations were made on samples cut by cryofracture from compressed disks similar to those used for the rheological measurements and coated with 50/50 gold/palladium.

Results and Discussion

1. Breaking Thread Method (BTM). The breaking thread method has been widely used to determine the interfacial tension in many polymer systems[9−11,18−20] such as LDPE/PA-6,[20] HDPE/PA-6,[10] PS/PA-6,[10,11,20] PP/LLDPE,[21] etc. This method is based on Tomotika's theory,[22] in which the interfacial tension is determined from the transient breakup of a long thread with time. The instabilities of the thread are governed by the local flow conditions and the rheological and interfacial properties of the fluids involved. Because of Brownian motion, local and small disturbances are generated at the surface of the thread. This leads to a pressure difference between the inside and the outside of the thread and then induces more important deformations caused by the effect of the interfacial tension that tends to reduce the interfacial area. When the wavelength (λ) of distortions is larger than the initial thread circumference ($2\pi R_0$), breakup of the thread occurs. This phenomenon was first observed by Plateau[23] and theoretically treated by Rayleigh[24] for inviscid fluids (known as Rayleigh instabilities). Later, Tomotika[22] extended the work of Rayleigh for two Newtonian fluids and established a theory to describe the kinetics of the thread fragmentation and to explain the experimental results obtained by Taylor.[25] Tomotika[22] assumed (i) incompressible Newtonian fluids, (ii) negligible inertial effects, (iii) symmetrical motion around the z axis of the cylinder, (iv) perfect adherence at the surface of the cylinder, (v) continuity of tangential stresses at the surface of the cylinder, (vi) the difference in normal stresses between the inside and the outside of cylinder is only due to the interfacial tension and obeys the Laplace Law, and (vii) no overall flow field is present (quiescent conditions). From his analysis, if the ratio of the viscosities of the two fluids is neither zero nor infinity, the breakup (maximum instability) always occurs at a certain definite value of the wavelength of the assumed initial disturbance. As shown in Figure 1, the analysis predicts that the distortion α grows exponentially with time

$$\alpha = \frac{b-a}{2d_0} = \alpha_0 e^{qt} \tag{1}$$

where d_0 is the initial diameter of the cylindrical thread, a_0 is the distortion magnitude at $t = 0$, and q is the growth rate of the sinusoidal distortion. The growth rate is directly related to the interfacial tension, γ_{12}, through

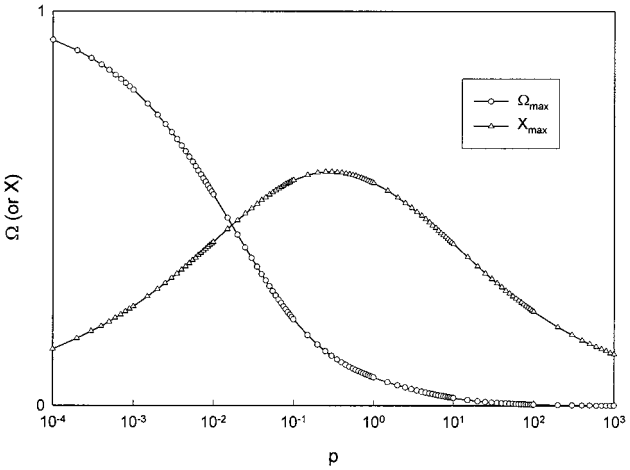

Figure 2. Dominant wavenumber, $x_m = 2\pi R_0/\lambda_m$, and dimensionless growth rate, $\Omega(x,p)$, as a function of the viscosity ratio of fiber polymer to matrix polymer, $p = \eta_d/\eta_m$.

$$q = \frac{\gamma_{12}\Omega(x,p)}{\eta_m d_0} \tag{2}$$

where p is the viscosity ratio ($p = \eta_d/\eta_m$), η_d and η_m are the viscosities of the thread and the matrix, respectively, x is the reduced wavelength of the distortion ($x = \pi d_0/\lambda$), and $\Omega(x,p)$ is a complex tabulated function of both the viscosity ratio (p) and the reduced wavelength (x). The interfacial tension is then determined from eqs 1 and 2. The time of breakup is given by[10]

$$t_b = \frac{\eta_m R_0}{\Omega(x,p)} \ln\left(\frac{1.39\gamma_{12}R_0^2}{kT}\right) \tag{3}$$

For a given viscosity ratio, there is a corresponding dominant reduced wavelength of distortions and a value for $\Omega(x,p)$. When the experimental reduced wavelength of distortions is close to the theoretical value, the experimental result can be considered as reliable. The theoretical wavenumber x_m ($x_m = \pi d_0/\lambda_m$) and $\Omega(x,p)$ are given as a function of the viscosity ratio (Figure 2). The values of $\Omega(x,p)$ can be calculated from Tomotika's original equation. When $p \to 0$, $\Omega(x,p)$ approaches unity. From Figure 2 for a given viscosity ratio, the corresponding theoretical reduced wavelength indicates that the dominant wavelength (λ_m) is a function of the diameter of the fiber. So, there will be a dominant wavelength, corresponding to a diameter, at which the amplitude grows the fastest and leads to the breakup of the thread into droplets.

Generally, the polymer with the highest melting point or glass transition temperature is used for the fiber. In this way, when the fiber is placed between the two films of the second polymer, the film is first softened, which provides a good imbedding of the fiber into the matrix by keeping the shape of the fiber. In the present work, the thread was made from PA-6. Typical optical micrographs of the distortions of PA-6 thread in the PS matrix at 230 °C are shown in Figure 3. The regularly spaced distortions, which appeared on the thread, lead to their disintegration into spheres within about 10 min. The diameter of the final spheres is approximately 2 times larger than that of the original thread, which is in

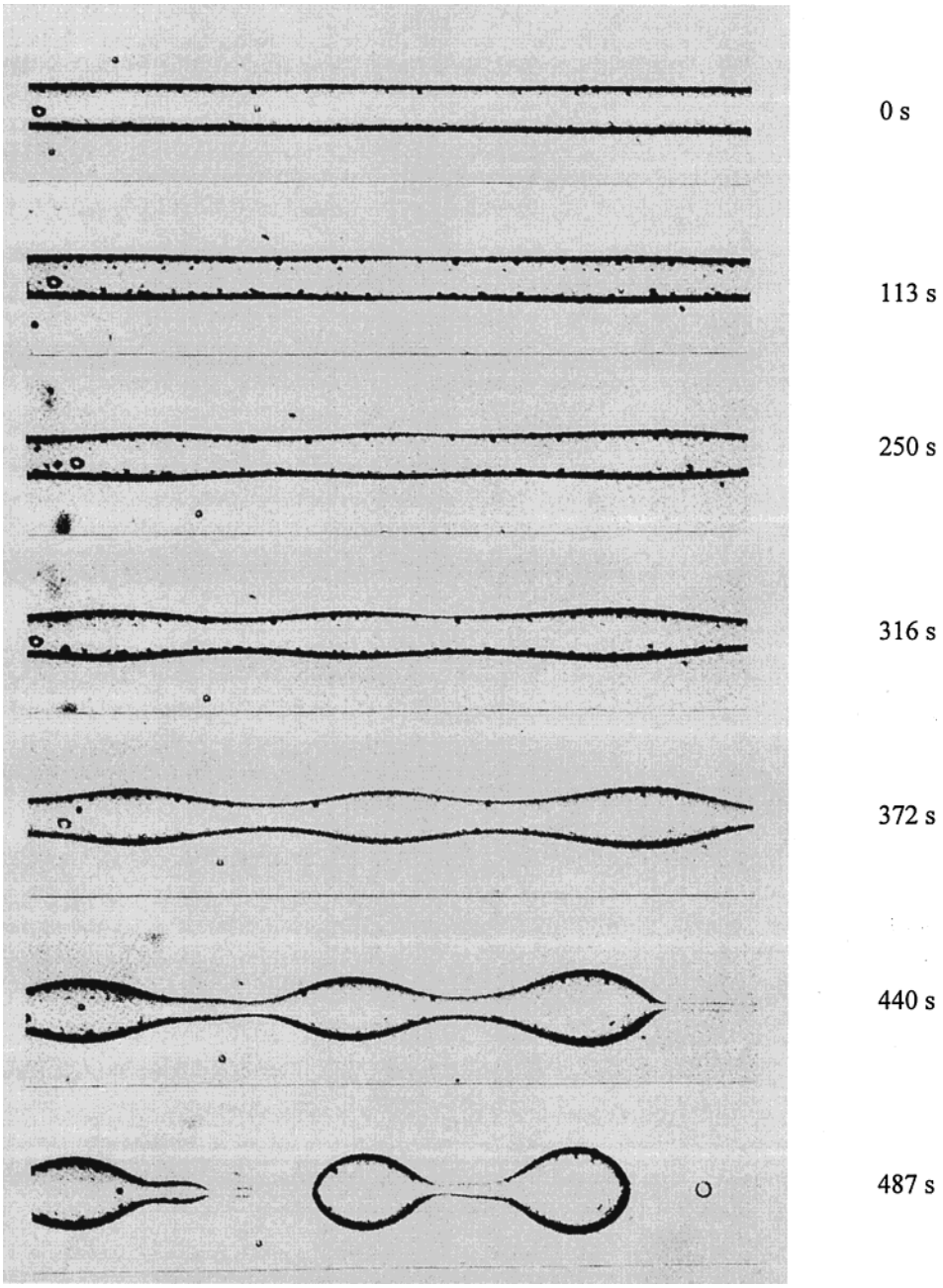

Figure 3. Optical microscope picture as a function of time of the growth of distortions of PA-6 fiber ($d_0 = 51.9\ \mu$m) in PS matrix at 230 °C.

accordance with the predictions of Tomotika's theory. Figure 4 shows the typical plots of log(α) versus time for four samples. The q values can be simply calculated from the slope of the curves (see eq 1). It is important to compare the theoretical dominant wavenumber with the experimental one. If the values of x_{max} and x_{exp} are close (within 10%), $\Omega(x,p)$ can be obtained using the dominant wavelength and the viscosity ratio. This value can then be used to calculate γ_{12} . In our experiments, the viscosity ratio was 1.08, for which x_{max} and Ω_{max} take the values 0.559 and 6.856×10^{-2}, respectively. The results of several experiments are reported in Table 2. Two types of results are reported: (i) with annealing of the thread and (ii) without annealing of the thread. Clearly, when the thread is not annealed, higher values of the interfacial tension are obtained. For annealed samples, the data are lower. Even though the data are relatively dispersed, a mean value of 8.4 ± 1.5 mN/m is obtained. This value is very close to the previously reported values of 7.3 mN/m (240 °C) by Cho et al.[11] and 6.3 mN/m (230 °C) by Luciani et al.[20] measured via the breaking thread method. However, this value is much lower than that reported by Elemans et al.[10] (20 mN/m). Generally commercial polymers have different molecular weight distributions and contain different additives such as stabilizers, antioxidants, and lubricants that can affect the measurements of the interfacial tension. All small molecular additives and the polymer chains with the lowest molecular weight in the case of broad molecular weight distribution prefer to migrate to the interface between polymers and lower the interfacial tension.

We should however point out that the data even with annealing are scattered widely, although they range in the interval 6−11 mN/m (Table 2). The difference between the lowest and the highest values is about 5 mN/m, which represents a 35% deviation from the mean value.

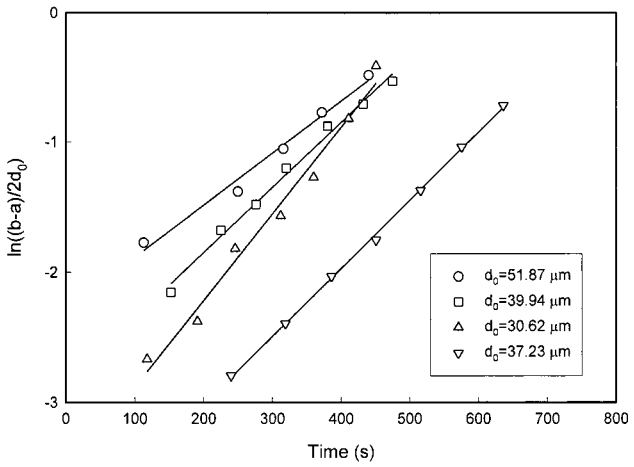

Figure 4. Dependence of the amplitude of distortions on the evolution time for PS/PA-6 at 230 °C.

Table 2. Interfacial Tension Values of PS/PA-6 at 230 °C Obtained from BTM

matrix	thread	d_0 (μm)	q ($\times 10^3$)	x	Ω ($\times 10^2$)	γ_{12} (mN/m)
PS	PA-6					
nonannealed		35.77	8.99	0.552	6.855	11.74[a]
fiber		38.46	15.50	0.570	6.852	21.84[a]
		40.52	9.54	0.518	6.796	14.21[a]
		42.13	8.06	0.578	6.841	12.56[a]
annealed PA-6		22.73	10.52	0.591	6.818	8.77
fiber		23.60	12.55	0.594	6.810	10.87
		30.62	6.65	0.514	6.785	7.51
		35.09	7.86	0.618	6.690	10.30
		37.23	5.23	0.571	6.851	7.11
		37.83	5.85	0.569	6.852	8.07
		38.38	5.89	0.580	6.839	8.26
		39.94	4.99	0.554	6.855	7.26
		42.37	3.78	0.609	6.765	5.92
		51.87	4.00	0.519	6.801	7.63
		54.95	5.17	0.502	6.729	10.55
				γ_{12} av		8.4
				SD		±1.5
				$\gamma_{12max} - \gamma_{12min}$		5.0

[a] These data were not included due to their residual stress.

Advantages of BTM. The "breaking thread" method has several advantages. At high temperatures, the process of thread breakup can occur in a reasonable period of time (several minutes to several hours) and thus reduces the eventual thermal degradation of the polymers. The experimental time can be varied through the change of the diameter of the thread, because a thread with a smaller diameter will break in a shorter time. The preparation of the samples is not very difficult. This method does not require the density values for the components, as is the case for the pendant drop method. Even for a polymer pair with very small density difference, which is difficult to measure in the pendant drop method, the BTM method can be used to estimate the interfacial tension. The technique does not require sophisticated apparatus.

Although the theory was derived for purely Newtonian fluids, the analysis is still valid for the majority of viscoelastic fluids, since the rates of deformation involved during the slow breakup process are on the order of $10^{-3}-10^{-2}$ s^{-1}.[9] In this range of rate of deformation, the majority of the polymers are in their terminal zone and behave as purely Newtonian fluids. However, one must verify that the time of breakup (see eq 3) is long compared to the terminal relaxation times of the components ($\eta_0 J_0^e$).

Limitations of BTM. This method has some limitations. It requires that the polymer matrix should be transparent, to allow visualization of the thread breakup. The method is also not suitable for polymer pairs with comparable softening temperatures (T_g for amorphous polymers or T_m for semicrystalline polymers). In this case, it is difficult to immerse the thread into the matrix melt while maintaining a good shape. Thus, a regular melt thread cannot be formed. Theoretically, the method is suitable for any viscosity ratio, but practically it is not suited for very large or very small viscosity ratios. If p is very small, it will lead to thread flattening, and a good thread immersion into the matrix cannot be obtained. If p is very large, a very long time is needed to complete the measurement, and eventual thermal degradation at high temperatures may take place.

The ratio of L/D of the thread should be high enough to be considered as an infinite cylinder (typically more than 50). If L/D is not very high, the thread will retract rather than breaking up, or the breakup will be affected by end effects (end pinching) rather than by spatially periodic capillary instabilities.[26,27] In our experiments L/D was about 300.

The technique excludes highly elastic materials and materials that are cross-linked. (Some of polymers can cross-link during the experiment by thermal effects.) In this case, elastic effects have to be taken into account, and more elaborate models such as Lequeux−Palierne's model[28] have to be used. The results can also be affected by the high orientation that may be introduced during preparation or by a particular anisotropic structure that may be present in the thread, as in liquid crystalline polymers (LCP).[20] This is because the orientation of polymer chains (especially in the LCP thread) affects the fluid circulation in the thread, which may affect the propagation of the disturbances along the thread. (Theoretical analysis of fluid circulation in this kind of structure can be found in the paper of Bousmina.[29]) Moreover, if the LCP is shear thinning (the majority of cases) in the entire shear region and exhibits a transient flow behavior, Tomotika's theory becomes invalid.

Experimental Difficulties with BTM. Various factors can introduce errors in the BTM. The first one is the residual stresses in the thread produced during the drawing from the molten pellet. If some residual stresses are present, the thread will distort faster (relaxation of residual stresses), and this will lead to interfacial tension values much higher than the real one. (The interfacial tension scales as the inverse of the rate of distortion; see eq 2.) This can be clearly seen in Table 2, where the values of γ_{12} can be 3 times larger (21.8 mN/m) than the average value (8.4 mN/m) extracted from the results obtained with annealing.

Different measurements are needed to determine the average value. Although very careful experiments we carried out, it was not possible to obtain a very narrow data distribution.

The initial thread should have a uniform shape and diameter. The diameter of the thread should be in the range 20−100 μm. A thread with smaller diameter will give larger errors, because the relative error in determining the diameter will be larger.

If the thread is not uniform, the distortion and breakup will take place quickly in zones with the smallest diameter or curved shape. In this case, it is not possible to obtain a uniform wavelength. The end pinching[10] phenomena or fiber retraction (as shown in

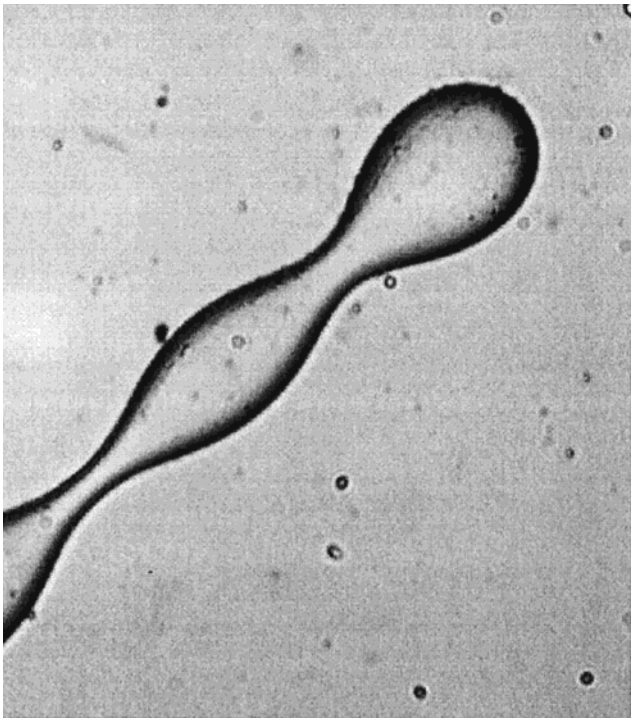

Figure 5. Distortions of PA-6 thread with nonuniform diameter in the PS matrix at 230 °C.

Figure 5) take place after the breakup at smallest diameter part of the thread. Then, it affects or even prevents the distortion of the nearest distortion of the thread. So a valid estimation of the interfacial tension cannot be obtained. This can also occur if air bubbles or impurities are present at the surface or in the neighborhood of the thread (at distance comparable to or less than the diameter of the resulting drops). The effect of impurities is, however, common to all techniques except to some extent for the rheological technique, where the presence of few impurities has negligible effect compared to the behavior of the two bulk polymers.

2. Imbedded Fiber Retraction Method (IFRM). The imbedded fiber retraction method (IFRM) is a dynamic method developed by Cohen and Carriere et al.[13,14] for measuring the interfacial tension between two polymer melts. It has been successfully applied to several polymer pairs such as PMMA/PS,[13,14,30] PC/PMMA,[15] PC/PE,[31] PP/polyolefin elastomer,[32] PP/PA-6,[33] and PC/PVDF.[34]

The technique is similar to the BTM, but here, due its short length, the imbedded fiber will retract to a spherical shape rather than breaking up. During this relaxation process, the fiber first transforms to a dumbbell-like intermediate shape by surface smoothing, then relaxes, and recovers an equilibrium spherical shape. Since the interfacial tension is the driving force for the retraction process, it can be evaluated from the rheological characteristics and from the transient modification of the dimensions of the fiber to the sphere.

This method is based on the simple balance between the interfacial and viscous forces at the fiber/matrix interface

$$6\pi\chi R(t)\eta_e \frac{1}{2}\frac{dL}{dt} = -\gamma_{12}\frac{dA}{dL} \tag{4}$$

where χ is a hydrodynamic empirical coefficient (usually equals 1),[14] $R(t)$ is the effective radius of the fiber, η_e is the effective viscosity, L is the length of the fiber, and γ_{12} is the interfacial tension.

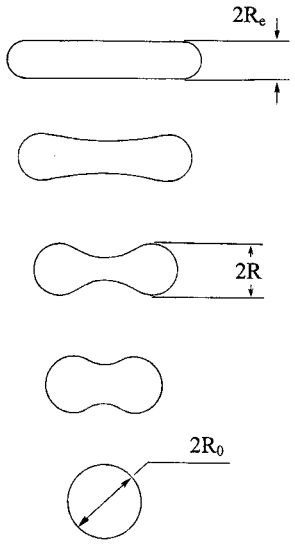

Figure 6. Schematic representation of the interfacial tension measurements by the imbedded fiber retraction method (IFRM).

The technique assumes that the fiber is a cylinder with hemispherical caps and an effective radius R during the retraction process. The effective radius R at time t is determined as the radius of a cylinder having equal volume and length as the fiber. A representative retraction process of imbedded fiber is shown in Figure 6. At the end of the process, the fiber will retract into a sphere with radius R_0. The final expression is

$$f\left(\frac{R}{R_0}\right) - f\left(\frac{R_e}{R_0}\right) = t\,\frac{\gamma_{12}}{R_0\eta_e} \tag{5}$$

where the R_e is the radius of the fiber at time $t = 0$.

The expression of the function f obtained by Cohen and Carriere et al.[14] has the form

$$f(x) = \frac{3}{2}\ln\frac{\sqrt{1+x+x^2}}{1-x} + \frac{3^{1.5}}{2}\arctan\left(\sqrt{3}\,\frac{x}{2+x}\right) - \frac{x}{2} - \frac{4}{x^2} \tag{6}$$

The effective viscosity was expressed by eq 7 empirically in ad-hoc manner as[14]

$$\eta_e = \frac{\eta_m + 1.7\eta_d}{2.7} \tag{7}$$

where η_m and η_d are the zero-shear viscosities of the matrix and the fiber, respectively. The interfacial tension is calculated from the slope of the curve $f[r(t)] - f[r(0)]$ versus the retracting time (see eq 5), where $r(t) = R(t)/R_0$.

According to the results of the breaking thread experiments, the breaking of PA-6 fiber in PS at 230 °C takes place at around $L/D \sim 12$ (but without uniform distortions). To avoid the breaking of the fiber, the ratio of L/D of PA-6 fiber was chosen from 7 to 12. R_0 can be calculated from the measurement of the initial fiber volume (V) ($R_0 = (3V/4\pi)^{1/3}$) according to the volume conservation. In this way, the experimental time can be greatly reduced, since only the transient regime is

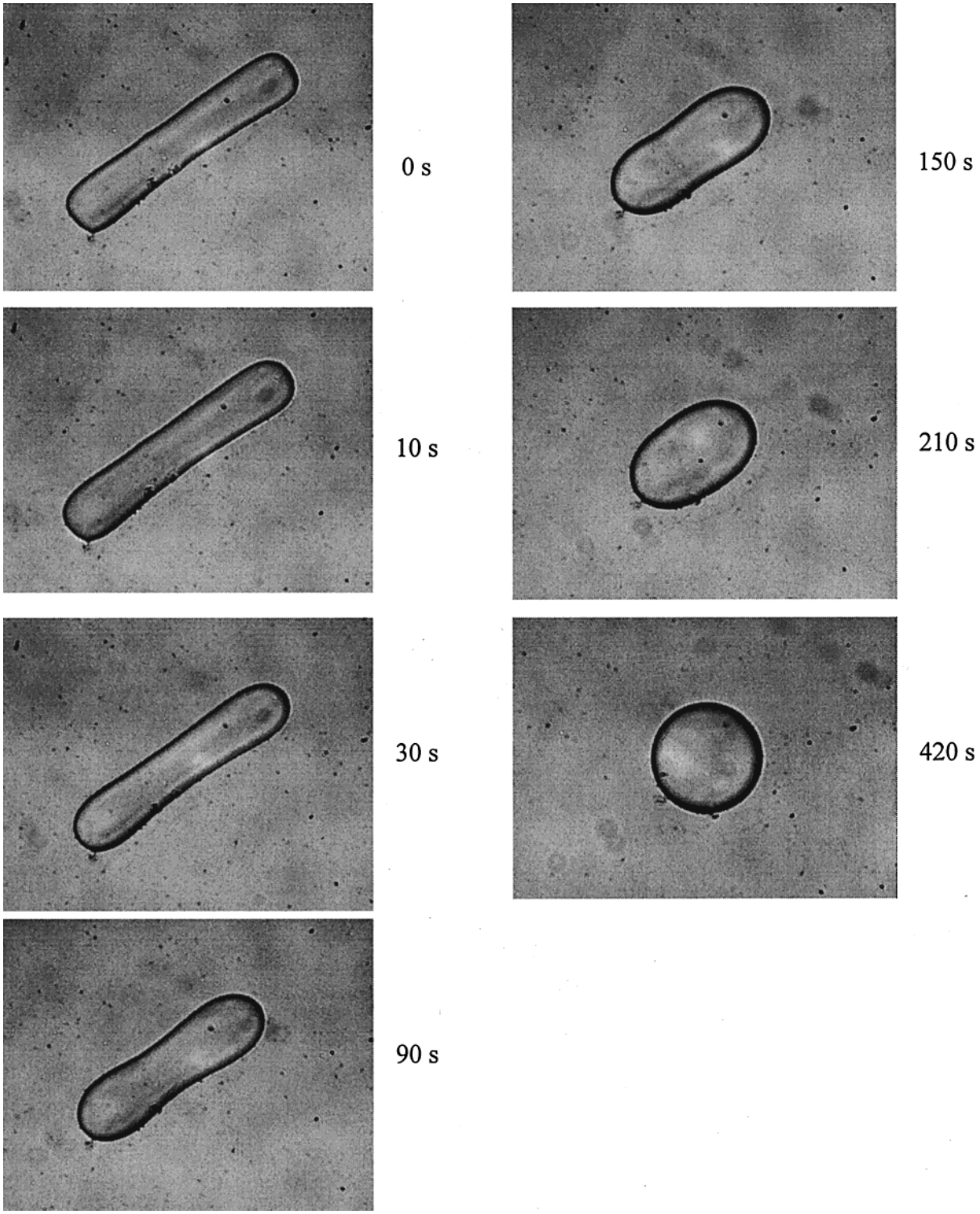

Figure 7. A typical optical micrograph of the fiber retraction of PA-6 imbedded in a PS matrix.

required. There is no need to reach the final steady-state spherical shape. However, in our experiments, the fiber retraction of PA-6 in PS melt can be completed within 10 or 20 min. So, the radius R_0 was directly measured from the final sphere. In this way, the error in measuring the volume can be avoided, because the fiber was made by drawing from the melted PA-6 pellet, so the symmetrical section of the fiber cannot be exactly the same. At the beginning of the experiment, the real fiber shape in the molten state is not the same as the initial solid fiber, and the starting time was not calculated from the beginning of the melting of the fiber. In fact, when the PA-6 fiber melts after the softening of the PS matrix, significant flattening occurs in the PA-6 fiber and then large retraction in the length takes place. After surface smoothing, the PA-6 fiber exhibits more uniformed shape, and thus the experimental time can be recorded from this point.

Typical optical micrographs for the retraction process of PA-6 fiber in the PS matrix at 230 °C are shown in Figure 7. The initial cylindrical fiber transforms to pronounced dumbbell shapes by decreasing the whole length. Then, with the retraction of the fiber, the central diameter increases and the dumbbell-like shape be-

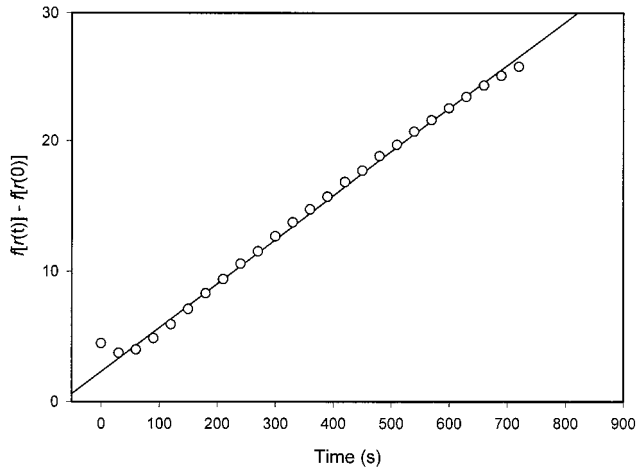

Figure 8. A typical plot of $f[r(t)] - f[r(0)]$ versus retraction time t for PA-6 fiber imbedded in a PS matrix.

Table 3. Interfacial Tension Values of PS/PA-6 at 230 °C Obtained from IFRM

matrix	fiber	L (μm)	R_0 (μm)	γ_{12} (mN/m)
PS	PA-6			
nonannealed fiber		563.76	79.74	11.77[a]
		662.05	75.31	14.44[a]
		709.84	73.56	13.21[a]
annealed fiber		591.36	81.90	6.83
		617.04	68.33	9.08
		663.78	86.70	7.39
		694.85	95.09	6.64
		709.86	89.45	8.19
		712.14	95.78	5.92
		741.21	108.92	8.64
		750.47	89.62	5.45
		756.92	82.12	7.27
		763.77	75.24	9.94
		γ_{12} av		7.5
		SD		±1.4
		$\gamma_{12max} - \gamma_{12min}$		4.5

[a] These data were not included due to their residual stress.

comes ellipsoidal before reaching the equilibrium spherical shape. A typical plot of $f[r(t)] - f[r(0)]$ versus retracting time is shown in Figure 8. The interfacial tension was determined from the slope of the curve (see eq 5).

The overall experimental results are reported in Table 3. It is clearly seen again that the results are higher when the fiber is not annealed. For annealed samples, the interfacial tension ranges in the interval 5−10 mN/m, with an average value of 7.5 ± 1.4 mN/m. The average value for nonannealed samples is 2 times higher.

Advantages of IFRM. One of the most important advantages of the technique is that it does not require the attainment of equilibrium. Only transient information is needed to calculate the interfacial tension, provided that the length and diameter can be accurately measured from the initial fiber. This reduces the experimental time and avoids thermal degradation.

Limitations of IFRM. The limitations of this method are that the matrix polymer should be transparent in the molten state and should be of lower softening point (T_g for amorphous polymer or T_m for semicrystalline polymer) than the fiber. This is for precise imbedding of the fiber in the matrix and to avoid the flattening of the fiber.

L/D should be lower than 12 to avoid breakup. The viscosity ratio p should be between 10^{-3} and 10^3. In this way, the fiber flattening and long experimental time can be avoided.

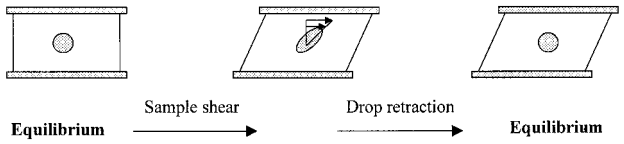

Figure 9. Schematic representation of the retraction of an ellipsoidal drop. The embedded PA-6 droplet is deformed by a displacement of the upper glass slide. The recovery rate of the PA-6 particle depends on the interfacial tension.

Experimental Difficulties with IFRM. Several precautions should be made to reduce the experimental errors. If the fiber is not in the horizontal plane after imbedding, important error will occur in the measurement of the fiber dimensions and can lead to large error in the final result. The equivalent viscosity given by eq 7 was empirically used by Cohen and Carrier et al. for PMMA/PS systems.[13,14] Rigorously, this ad-hoc equation cannot be used for other systems. However, since the technique requires only transient data, eq 7 can be replaced by eq 5 (Rallison equation[35] was derived theoretically), at the end of the process where the shape is more likely to be ellipsoidal. This implies that the IFRM reverts to the DDRM method (the final stage of the IFRM is in fact similar to the DDRM), and there is room for improving the theory using the same guidelines as for the DDRM method (see section 3).

The curved shape of the fiber or the residual stress will accelerate fiber retraction and give higher interfacial tension values (see eq 5).

3. Retraction of Deformed Drop Method (DDRM). In the BTM, it is not easy to prepare the thread with straight shape and uniform diameter. To overcome this limitation, the group of Utracki[12] has proposed a new dynamic method named the retraction of deformed drop method (DDRM). The method is based on the interfacial tension driven shape recovery of a slightly elongated drop. The quantitative treatment is based on Taylor[25] theory about the deformation of a viscous drop immersed in a second fluid submitted to steady shear flow at small amplitude of deformation. It is assumed that the recovery of the presheared drop is driven only by the interfacial tension and that the rheological properties of the polymers do not change during the measurements. The deformed drop retraction method (DDRM) allows the determination of the interfacial tension from the shape evolution of the deformed drop toward its equilibrium shape (Figure 9). The following expression was obtained for the deformation D:

$$D = D_0 \exp\left\{-\frac{40(p+1)}{(2p+3)(19p+16)}\frac{\gamma_{12}}{\eta_m R_0}t\right\} = D_0 \exp\left\{-\frac{t}{\tau_d}\right\} = \frac{L-B}{L+B} \quad (8)$$

where D_0 is the deformability parameter at t_0, p is the viscosity ratio of the dispersed to the matrix phase, and L and B represent the major and the minor axes of the ellipsoid, respectively. The relaxation time τ_d and the equivalent viscosity η_{eq} are defined as

$$\tau_d = \frac{\eta_{eq} R_0}{\gamma_{12}} \quad (9)$$

and

$$\eta_{eq} = \frac{(2p + 3)(19p + 16)\eta_m}{40(p + 1)} \quad (10)$$

From eqs 8 and 9, the interfacial tension (in the transient regime) can be determined using the time evolution of the deformed drop toward its equilibrium shape. In principle, the relations are only valid for Newtonian systems, but the method can also be used to characterize viscoelastic material in the case where the following two conditions are valid: (i) the deformation is small and retraction rate is sufficiently slow to ensure that the materials behave as Newtonian, and (ii) the elastic relaxation of the materials after deformation is faster than ellipsoidal droplet retraction.

A typical picture of the retraction process of a deformed PA-6 drop immersed in a PS matrix at 230 °C is illustrated in Figure 10. After cessation of shear, the ellipsoid relaxes and recovers its equilibrium spherical shape. The retraction is completed within 6 min. The central part of the ellipsoid was measured as the minor axis (B). Figure 11 shows a typical plot of the variation of the major axis (L) and the minor axis (B) of PA-6 ellipsoid in the PS matrix at 230 °C as a function of time. Because the major axis of the ellipsoid (L) has a small angle with the surface plane, the L value cannot be measured directly. It can be calculated from the B value, assuming symmetry of the ellipsoid and volume conservation ($L = 8R_0^3/B^2$). The deformability parameter, D, of the PA-6 drop can be calculated from this plot. This is shown in Figure 12. From the plot of the deformability as a function of time, the interfacial tension can be obtained using eqs 8−10. The set of experimental results is reported in Table 4. The interfacial tension varies in the interval 4−10 mN/m. As for the BTM, a large error can arise if measurements are carried out. The average value and standard deviation for our experiments is about 6.8 ± 1.8 mN/m.

Advantages of DDRM. The DDRM method has several advantages. The method is easy to handle, and sample preparation is very simple. It is not necessary to have during the initial step of generation of the drop a uniform thread and a uniform thread breakup; the only required condition is a well-defined and isolated drop. If problems of thermal degradation are not present, the technique can be used for systems with high viscosity (but not too high: see the limitations), where the other methods are not suited. For example, due to the high viscosity of HDPE, it is not possible to determine the interfacial tension of HDPE/PA-6 by the breaking thread method,[12] whereas the measurement is possible with the DDRM method. The experiments can be repeated several times using the same testing sample. This allows the verification of the method reproducibility and also the determination of the interfacial tension at different temperatures on the same sample. The method also gives the transient and the equilibrium interfacial tensions. This is a very important issue in polymer processing such as extrusion, especially in zones of small pressure gradient or in long dies at low extrusion speeds, where the morphology is controlled by transient interfacial tension rather than by the equilibrium values.

Limitations of DDRM. The limitations are related to transparency, droplet size, viscosity ratio, cross-linked drops, and LCP. Similar to the BTM, this method is rigorously not suitable for the polymer/LCP system, because recovery of the ellipsoid does not produce sphere, due to the molecular chain orientation of the LCP drop.

Experimental Difficulties with DDRM. The DDRM method has some difficulties that may produce some errors in the estimated values of the interfacial tension. First, it is difficult to apply the shear without imposing a certain pressure on the system when the upper slide is moved. New devices are now available which can apply a given shear with suitable shear rate and minimum pressure (Linkam sliding plates of Cambridge). Second, for highly viscous drops, the overall time needed to generate the drop by BTM of IFRM and the time required for retraction maybe too long. This may cause, at high temperatures, thermal degradation of the polymers. The small molecules produced from thermal degradation will reduce the interfacial tension when they migrate to the interface.

The expression used for the equivalent viscosity was given by the Rallison[35] theory for small deformation of a viscous drop in shear flow at low capillary number. This means that the difference between the major axis of the ellipsoid and the final radius of the relaxed drop should be small (few percent). This can introduce some errors, since it involves determination of the difference in the dimensions of two not very different parameters. It should also be pointed out that for large deformations without breakup other expressions should be used. For both low and high viscosity ratios, the deformation D takes on similar values

$$D = D_0 \exp\left\{-C \frac{\gamma_{12}}{\eta_i R_0} t\right\} \quad (11)$$

where C is a constant (close to 1) and η_i is the viscosity of the matrix (η_m for small p) or the viscosity of the drop (η_d for large p). If one considers the two following situations—(i) small p: $\eta_d = 10^2$ Pa·s and $\eta_m = 10^5$ Pa·s and (ii) large p: $\eta_d = 10^5$ Pa·s and $\eta_m = 10^2$ Pa·s—eq 8 gives the same magnitude for the relaxation time, which is not physically acceptable. However, the situation is different here due to the inability to deform the drop under high-p conditions. In fact, Grace[36] has shown that it is very difficult to deform (and break up) the viscous drop (dispersed in a viscous matrix) with $p > 4$, where the flow is mainly controlled by rotational flow rather than by shear.

The other difficulty is that the real length of the major axis of the ellipsoidal drop is calculated from the length of the minor axis, assuming perfect symmetry of the ellipsoid. If this condition is not satisfied, this will bring some errors in the calculation of the deformability parameter, and thus will affect the accuracy of the interfacial tension determination.

4. Pendant Drop Method (PDM). The pendant drop is widely used for the determination of the interfacial tension. The technique has been applied to many polymer pairs, such as PP/PS,[4,5,37] LDPE/PA-6,[19] HDPE/PS,[38] PS/PET,[38] and PS/PDMS,[39,40] etc. It consists of immersing a drop of one polymer in the matrix of another polymer. The interfacial tension is determined from the equilibrium shape of the drop profile and the difference between the densities of the two components

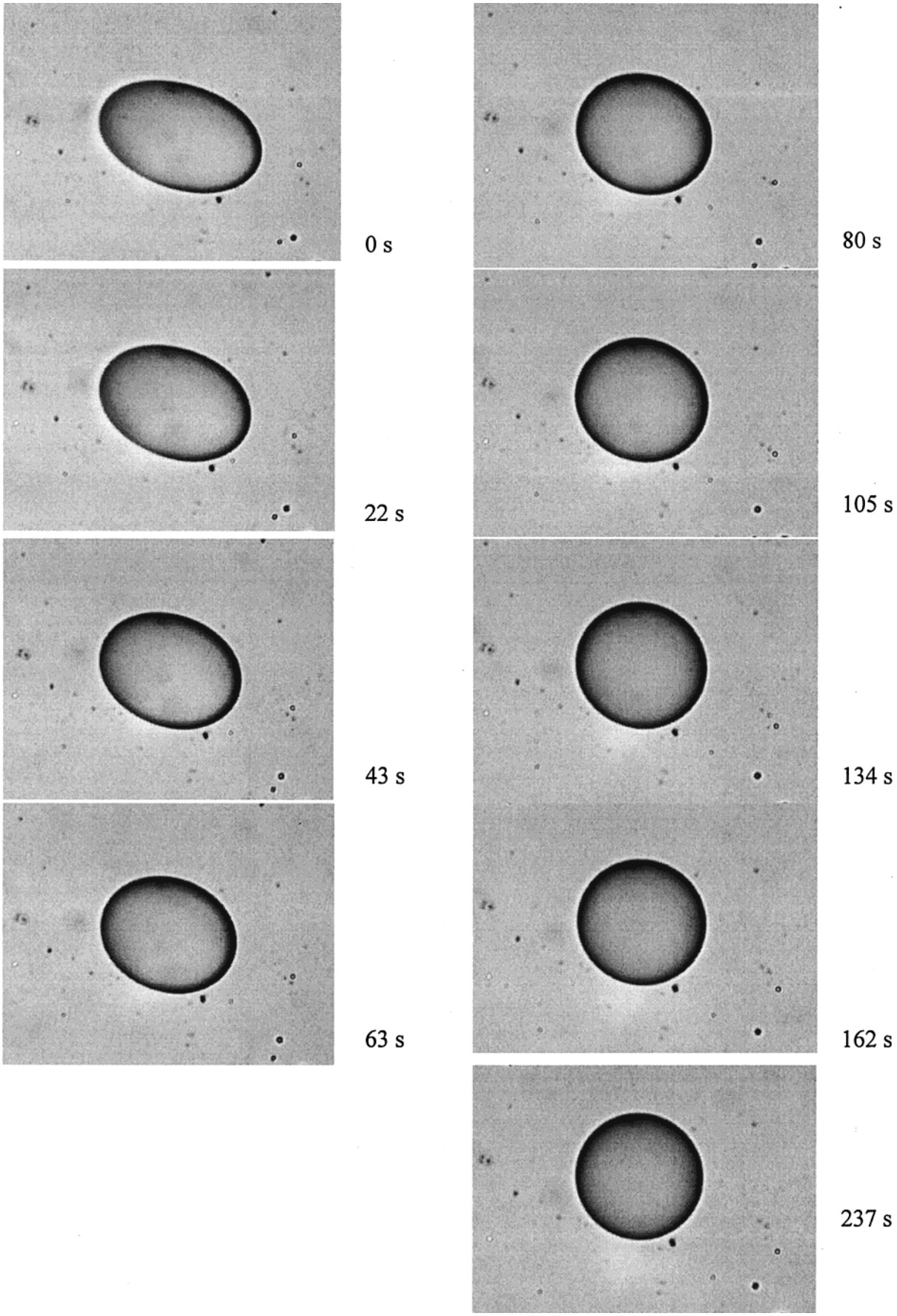

Figure 10. Retraction of a PA-6 ellipsoidal droplet immersed in PS matrix at 230 °C. The spherical particle radius is $R_0 = 73.60$ μm. Time of measurement is reported on each micrograph.

at the relevant temperature. The equations are based on the balance between gravitational and buoyancy forces between the drop liquid and the suspending medium. The mechanical equilibrium between the two

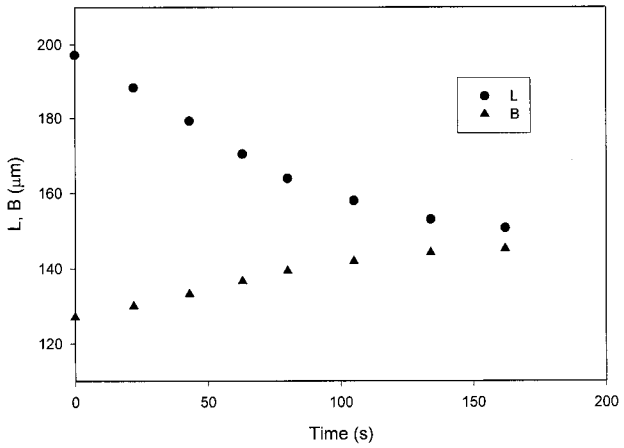

Figure 11. Time evolution of B and L for a PA-6 droplet immersed in a PS matrix at 230 °C. Values of L were calculated from B using a spherical droplet diameter $d/2 = R_0 = 73.60$ μm.

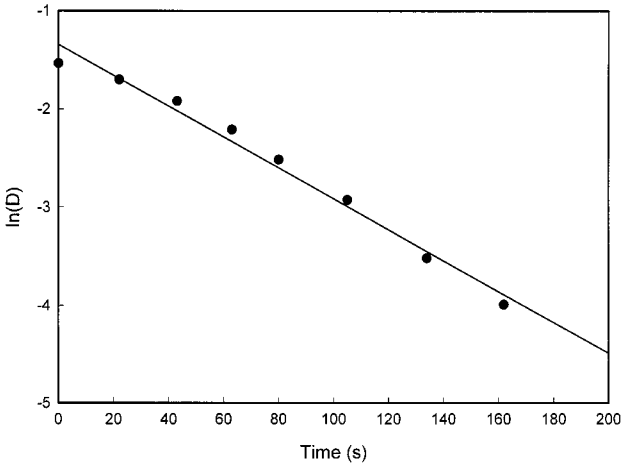

Figure 12. Deformability D versus time for a PA-6 ellipsoidal droplet immersed in a PS matrix at 230 °C.

Table 4. Interfacial Tension Values of PS/PA-6 at 230 °C Obtained from DDRM

matrix	droplet	R_0 (μm)	$1/\tau_d$ (s^{-1}) ($\times 10^2$)	γ_{12} (mN/m)
PS	PA-6	34.35	1.052	4.10
		47.35	1.611	4.33
		49.40	2.627	7.35
		53.51	1.732	5.25
		55.57	2.590	8.15
		58.62	3.061	10.16
		62.92	1.889	6.77
		72.10	2.182	8.91
		73.60	1.538	6.41
			γ_{12} av	6.8
			SD	±1.8
			$\gamma_{12max} - \gamma_{12min}$	6.0

liquids is given by the Laplace equation

$$\frac{1}{R_1} + \frac{1}{R_2} = \frac{\Delta P}{\gamma_{12}} \tag{12}$$

where R_1 is the principal radius of curvature in the plane and R_2 is the principal radius of curvature in a plane perpendicular to Figure 13; ΔP is the pressure difference across the curved interface, and γ_{12} is the interfacial tension.

R_2 is given by

$$R_2 = \frac{x}{\sin \phi} \tag{13}$$

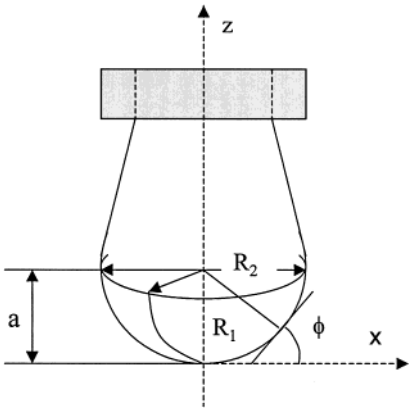

Figure 13. Schematic representative geometry of a pendant drop.

where ϕ is the angle between the radius of curvature R and the z-axis, and x is the abscissa, as shown in Figure 13. The pressure difference ΔP, across the interface at any vertical position, can be expressed as

$$\Delta P = \Delta P_0 + gz\Delta\rho \tag{14}$$

where g is the gravitational acceleration, $\Delta\rho$ is the density difference between the two polymer melts, and z is the ordinate along the z-axis. Equation 12 was rewritten by Bashforth and Adams[41] as follows

$$\frac{1}{R_1/a} + \frac{\sin \phi}{x/a} = B\frac{z}{a} + 2 \tag{15}$$

where a is the radius of curvature at the apex of the drop and B is a dimensionless quantity given by

$$B = \frac{\Delta\rho g a^2}{\gamma_{12}} \tag{16}$$

R_1 and ϕ can be determined from the drop profile by

$$R_1 = \frac{[1 + (dz/dx)^2]^{3/2}}{d^2z/dx^2} \tag{17}$$

$$\sin \phi = \frac{dz/dx}{[1 + (dz/dx)^2]^{1/2}} \tag{18}$$

The Bashforth and Adams equation is a nonlinear differential equation between x and z relating the drop profile to the interfacial tension. R, x, a, and z appear as ratios to the radius of curvature at the apex. The interfacial tension is then determined from the equilibrium profile (R_1 and sin ϕ) using eqs 15 and 16. In our experiments, the density difference for the two polymer melts (PS and PA-6 at 230 °C), calculated from the $P-V-T$ equations for PS[42] and PA-6,[43] is 0.0485 g/cm^3, which is small but still allows accurate estimation of the interfacial tension between PA-6 and PS.

In the present experiments, the equilibrium state of the pendant drop of PA-6 was reached after 17 h at 230 °C. A typical image of a PA-6 pendant drop at equilibrium is shown in Figure 14. Only two experiments were carried out with the pendant drop method. The interfacial tension obtained from these two individual ex-

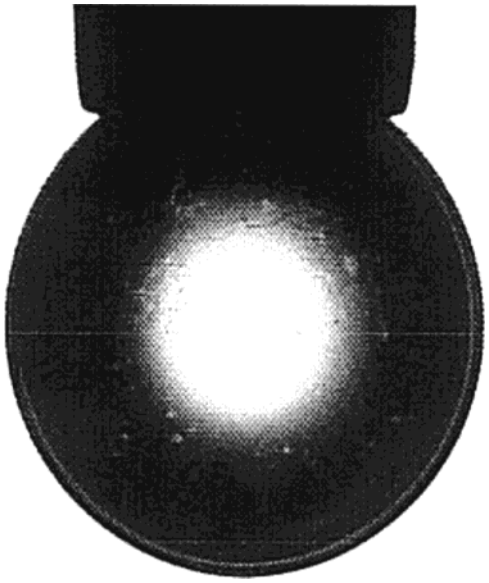

Figure 14. Typical pendant drop (digitized image) of PA-6 immersed in a PS melt at 230 °C.

periments gave almost the same values 7.15 and 7.27 mN/m, which gives an average of 7.2 ± 0.1 mN/m. Even though there are no reported interfacial tension value for the PS/PA-6 system using the pendant drop method, this value is quite close to the value obtained from the BTM, the IFRM, and the DDRM.

Advantages of PDM. This method is valid for both Newtonian and viscoelastic fluids. (No assumption about the rheological behavior of the component was made in the theory.) It can provide accurate measurements, and the error range is small. Since the interfacial tension is determined at equilibrium, the technique can be applied to LCP drops (the LCP should possess the highest density), where a priori the other methods are not valid, since during the transient regime, fluid circulation inside the dispersed phase (thread, drop, fiber) is highly influenced by the particular orientation inside the drop or thread.

Limitations of PDM. The technique has the following limitations: (i) the polymer matrix should possess the lowest density and must be transparent; (ii) the two polymers should have different densities at the working temperature, and the density difference should be larger than 4−5%, to reach the equilibrium shape in an acceptable interval of time to avoid thermal degradation. For a small density difference, the driving force is very small and sometimes makes it impossible to reach equilibrium and to determine the interfacial tension through this method.[38] (iii) During the experiment, the equilibrium state of the drop must be reached to make accurate measurements of the interfacial tension, because the Bashforth and Adams equation is only valid for a drop in its equilibrium state. The variables affecting the drop equilibrium time are the melt viscosity and the density difference between the two polymers, the initial drop volume, and the interfacial tension value. For low-viscosity liquids such as water, the equilibrium state is almost instantaneous.[44] In contrast, for polymers, due to their high viscosity and long relaxation time, the drop requires several hours or even several tens of hours to reach the equilibrium state; in this case, it may not be possible to carry out measurements due to thermal degradation.

Experimental Difficulties with PDM. In this method, several factors may bring errors in the final results. It is important to have an axisymmetric drop in order to obtain a reliable value for the interfacial tension. Drop asymmetry causes a decrease in the pressure difference and in the curvature.[45] The apparent inconsistency between the decreases in the curvature and the pressure difference terms leads to lower values for the interfacial tension (see eqs 15 and 16).

In this method, the interfacial tension is determined on the basis of drop shape fitting. Thus, drops with small volume will be associated with larger error in the final result, because curve fitting involves only part of the drop. Thus, it is desirable to maximize the volume of the drop. A critical volume can be determined by producing drops with different volumes by changing the initial extruded drop volume. If the drop is found unstable after a long measurement time, a smaller volume of the drop should be tested. When the drop profile becomes stable, it can be used to determine the interfacial tension. In our work, the comparison was facilitated by the on-line digital image analysis that compares the shape of the drop at different times. The critical drop volume for PA-6 in PS matrix was found to be of around 21 mm^3.

Since the interfacial tension is determined at equilibrium, a long experimental time at high temperature can easily induce thermal degradation of the polymers. In our case, weight loss at 230 °C under a nitrogen gas atmosphere during 17 h was 1.5% and 1.1% for PS and PA-6, respectively, as obtained by TGA measurements. The small molecules produced by the thermal degradation of the polymers may prefer to migrate to the interface and thus reduce the interfacial tension. The specially designed pendant drop device used in this work helps to minimize the experimental time. The video camera and the digital image acquisition and processing system allow on-line computations, which leads to a rapid estimate of the transient interfacial tension. This gives continuous monitoring of the transient interfacial tension values and permits the reduction of the experimental time by extrapolation of the transient values.[4]

5. Rheological Method (RM). Small-amplitude oscillatory measurements are known to be of pertinent use in capturing relaxation of drops in polymer blends. Immiscible molten polymer blends show an increase in elasticity (secondary plateau in G') at the low-frequency range and long time relaxation compared to that of the pure components. Several studies have shown that such a phenomenon is related to the slight deformation and shape relaxation of the dispersed drops caused by the interfacial tension.[29,46−51] Two emulsion models, Palierne's model[47] and Bousmina's model,[29] were used in this work to extract the interfacial tension from the experimental dynamic moduli, G' and G''. For a blend with particles of uniform size, Palierne's model[47] expresses the complex shear modulus of the blend, G_b^*, as a function of the complex shear moduli of the phases (G_m^* for the matrix and G_d^* for the dispersed phase), the volume fraction, ϕ, and the ratio of the interfacial tension and the size of particles (supposed here to be uniform in size), γ_{12}/R.

$$G_b^*(\omega) = G_m^*(\omega)\frac{1 + 3\phi H(\omega)}{1 - 2\phi H(\omega)} \qquad (19)$$

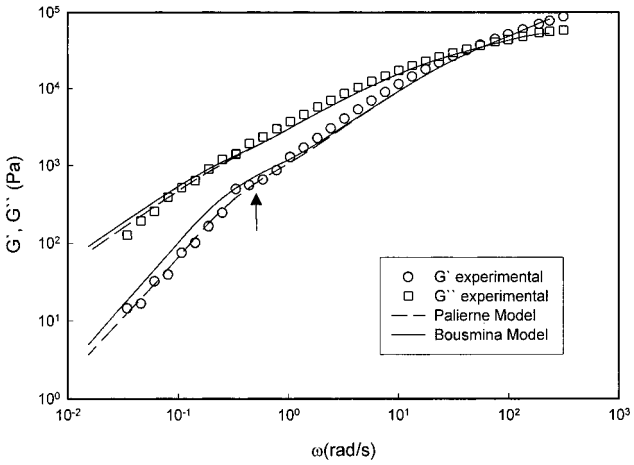

Figure 15. Typical plots of the experimental and model predicted dynamic moduli versus frequency for a 80/20 PS/PA-6 blend. Palierne model with $\gamma_{12} = 7.1$ mN/m and Bousmina model with $\gamma_{12} = 7.0$ mN/m.

where

$$H(\omega) = \{4(\gamma_{12}/R)[2G_m^*(\omega) + 5G_d^*(\omega)] + [G_d^*(\omega) - G_m^*(\omega)][16G_m^*(\omega) + 19G_d^*(\omega)]\}/\{40(\gamma_{12}/R)[G_m^*(\omega) + G_d^*(\omega)] + [2G_d^*(\omega) + 3G_m^*(\omega)][16G_m^*(\omega) + 19G_d^*(\omega)]\} \quad (20)$$

Bousmina's model[29] expresses the complex shear modulus of the blend as a function of the same parameters by

$$G_b^*(\omega) = G_m^*(\omega) \times \frac{2\left[G_d^*(\omega) + \frac{\gamma_{12}}{R}\right] + 3G_m^*(\omega) + 3\phi\left[G_d^*(\omega) + \frac{\gamma_{12}}{R} - G_m^*(\omega)\right]}{2\left[G_d^*(\omega) + \frac{\gamma_{12}}{R}\right] + 3G_m^*(\omega) - 2\phi\left[G_d^*(\omega) + \frac{\gamma_{12}}{R} - G_m^*(\omega)\right]} \quad (21)$$

The two models were worked out for viscoelastic incompressible emulsions undergoing small amplitude of deformation (linear viscoelasticity). The two models have been shown to give quite similar results for usual polymer blends,[29,50−52] but they differ for blends with structured drops such as LCPs. (Such a structure is taken into account by Bousmina's model.)

The two models do not contain any fitting parameters, and all of the parameters are experimentally accessible. In the case where the interfacial tension is not known, the two models can lead to an estimation of its value by fitting the theoretical curves to the experimental data. The value of the interfacial tension is taken as the value giving the best fit to either equation. Such a fit for the two models is shown in Figure 15. The average radius of the particles appearing in the two models was determined from SEM micrographs of PS/PA-6. The results obtained for two compositions PS/PA-6 80/20 and 90/10 are listed in Table 5.

There is not much difference in the fitting results obtained from the two models, which give quite similar interfacial tension values.

Advantages of RM. The two models have the advantage of being generally applicable to viscoelastic blends in the molten state. The models also provide a more realistic evaluation of the role of the interfacial tension, since the behavior is averaged over the total interface in the blend rather than considering only one drop, one thread, or one fiber. The Bousmina model takes into account of the anisotropic behavior of dispersed drops, and thus, in principle, it can be applied to polymer systems containing LCP drops, in which case other methods may be questionable.

Table 5. Experimental Results from the Data Fitting to the Palierne and Bousmina Models

	PS/PA-6 (90/10)	PS/PA-6 (80/20)	av γ_{12} (mN/m)
radius (μm)	1.99	2.22	
Palierne model	7.3	7.1	7.2 ± 2.0
Bousmina model	7.2	7.0	7.1 ± 2.0

Table 6. Comparison of Interfacial Tension Measured in This Work with Data Reported in the Literature for PS/PA-6 Using Various Methods

method	this work (mN/m)	lit. data (mN/m)	ref
BTM	8.4 ± 1.5	6.3	20
		7.3 (240 °C)	11
		20	10
IFRM	7.5 ± 1.4		
DDRM	6.8 ± 1.8		
PDM	7.2 ± 0.1		
Palierne model	7.2 ± 2.0		
Bousmina model	7.1 ± 2.0		

Limitations of RM. The technique can be used only if the secondary plateau in G' is experimentally accessible, depending on the torque and the frequency range of the rheometer. This depends on the viscosity ratio, the particle size, and the volume fraction of the dispersed phase. For very high viscosity ratio, the relaxation time may be very high and the terminal zone is shifted to very low frequencies. These may not be accessible experimentally due to the limitation of the frequencies available on the rheometer. If the size of the particles is very small or the volume fraction is small, it is difficult to obtain a well-defined secondary plateau at low frequencies, which may be useful for an accurate fit.

Experimental Difficulties with RM. The rheological technique presents some difficulties. It requires preparation of the blends by mechanical mixing or in solution, and the size of the particles has to be determined by electron microscopy. The error made in the estimation of the particle size affects directly the determination of the interfacial tension, because the two parameters R and γ_{12} appear in the two models as the ratio γ_{12}/R. Some errors can also originate from the fitting procedure. These errors may be difficult to assess in a unique manner, if the secondary plateau in G' is not well defined.

Concluding Remarks

In this work, we have compared five experimental techniques for the determination of the interfacial tension in polymer blends using a PS/PA-6 model system as a base for comparison. Each technique is based on a balance between a driving force and a resistance force. The dynamic methods (BTM, IFRM, and DDRM) are based on the balance between the interfacial forces and viscous forces, the equilibrium method (PDM) is based on the balance between the interfacial forces and gravitational forces, and the rheological methods are based on the balance between shear stress and interfacial forces.

Table 7. Summary of the Different Experimental Methods

method	advantage	limitation	difficulty
BTM	short measurement time	polymer matrix must be transparent	straight thread with uniform diameter and well immersed in matrix melt
	does not require the density values	viscosity < 10^5 Pa·s for both polymers	
	requires simple tools	does not take into account viscoelasticity	requires clean samples without impurities nor bubbles
		not valid for polymers with close softening points	
IFRM	short test time	polymer matrix must be transparent	straight thread with uniform diameter and well immersed in matrix melt
	valid for high viscosity systems	empirical equation	
	does not require the density values	viscosity ratio must be between 10^{-3} and 10^3	requires clean samples without impurities nor bubbles
	requires simple tools	not valid for polymers with close softening points	
DDRM	short test time,	polymer matrix must be transparent	well-deformed drop with symmetrical section
	repeated measurements on the same sample	viscosity ratio should be lower than 4	requires clean samples without impurities nor bubles
	easy to prepare samples	does not take into account viscoelasticity	
	requires simple tools		
PDM	accurate interfacial tension value	long experimental time	difficult to obtain accurate density values of both polymer melts
	valid for Newtonian and viscoelastic fluids	polymer matrix must be transparent and possess the lowest density	possible thermal degradation for highly viscous polymers
RM	valid for viscoelastic system	limited by the torque and frequency accessible with the rheometer	difficult to obtain accurate diameter of the dispersed drops
	valid for high viscosity system		many step experiments are required
	results are obtained on several droplets rather than a unique isolated droplet	limited to small deformation flow (linear viscoelasticity)	
		limited to spherical shape of the dispersed particles	

Table 6 shows the interfacial tension values obtained from these five methods. Even though the difference between the highest and the lowest values is not small (1.6 mN/m), a 20% difference between them is reasonable and acceptable. In our case, the experimental error increases in the following order: equilibrium method < dynamic method < rheological method.

The main objective of the present study was to evaluate and compare experimentally all of the above methods. To do so, we presented the theoretical bases of each method and we discussed the advantages, limitations, and difficulty that can arise during the experimental manipulations. Table 7 gives an overview of the five methods presented. Each technique has some advantages and some limitations, and the selection of a suitable method depends on physical properties such as viscosity, viscosity ratio, matrix transparency, elasticity, and softening points.

The IFRM, DDRM, and RM can be used to measure the interfacial tension of polymers with high viscosity (about 10^5 Pa·s) where the BTM and PDM are not suitable in this case, due to long experimental time. The BTM and the IFRM are also not suitable to measure the interfacial tension of polymer pairs with similar softening points (T_g for amorphous or T_m for semicrystalline polymers) due to the difficulty in preparing the samples. The BTM, IFRM, DDRM, and PDM all require that the polymer matrix must be transparent in the molten state and that the contrast between the two phases must be high with a good definition in order to make accurate measurements.

The greatest advantage of the three dynamic methods is the short time required to complete the experiments, thus avoiding thermal degradation of the polymers. Furthermore, the time can be adjusted through a change of the diameter or the length. In contrast, the PDM method is not suitable for readily degradable polymers, because several hours or even several days may be needed to reach the equilibrium state for highly viscous polymers. However, the PDM method can provide excellent reproducibility and accuracy of the data compared to the other methods. The main source of the errors is related to the fitting of the drop profile and to the measurement of the density difference between the two polymer melts.

Table 8. Comparison between Each Method

method	experimental time	sample preparation	error range
BTM	3	3	3
IFRM	2	2	2
DDRM	1	1	4
PDM	5	5	1
RM	4	4	5

The most important advantage of the RM (Palierne and Bousmina models) is that it takes into account the viscoelastic behavior of the polymers, and the data are representative of the total interfacial area. This is because the interfacial tension is determined from the shape relaxation of several drops rather than a unique isolated drop. The technique is however limited by the torque and the frequency range accessible on the rheometer. If the shoulder on the elastic modulus is not well defined, large error can be made in the determination of the interfacial tension.

To complete the comparison between the different methods, we provide in Table 8 a ranking from 1 to 5 for each method. The different bases for ranking are the time needed to perform the experiment, the difficulty attributed to the preparation of the sample, and the error range expected for the results. Generally, the error

range is inversely proportional to the difficulty and experimental time needed. However, we should point out that even though the results of this study provide general guidelines for selecting the most suitable method for a given sample system, our conclusion however was rigorously restricted to the system we investigated. A general conclusion requires more systems (different densities, different viscosity ratio, transparency, molecular weight distribution and temperature, etc.)

Acknowledgment. The authors acknowledge the help of Mr. Kevin Alam for the pendant drop experiments and also acknowledge the financial support from FCAR and NSERC.

References and Notes

(1) Wu, S. *Polymer Interface and Adhesion*; Marcel Dekker Inc.: New York, 1982.
(2) Adamson, A. W. *Physical Chemistry of Surfaces*, 3rd ed.; John Wiley & Sons: New York, 1982.
(3) Anastasiadis, S. H.; Chen, J. K.; Koberstein, J. T.; Siegel, A. F.; Sohn, J. E.; Emerson, J. A. *J. Colloid Interface Sci.* **1987**, *119*, 55.
(4) Demarquette, N. R.; Kamal, M. R. *Polym. Eng. Sci.* **1994**, *34*, 1823.
(5) Kamal, M. R.; Lai-Fook, R.; Demarquette, N. R. *Polym. Eng. Sci.* **1994**, *34*, 1834.
(6) Coucoulas, L. M.; Dawe, R. A. *J. Colloid Interface Sci.* **1985**, *103*, 230.
(7) Patterson, H. T.; Hu, K. H.; Grindstaff, T. H. *J. Polym. Sci., Part C* **1971**, *34*, 31.
(8) Joseph, D. D.; Arney, M. S.; Gillbert, G.; Hu, H.; Dulman, D.; Verdier, C.; Vinagre, T. M. *J. Rheol.* **1992**, *36*, 621.
(9) Elmendorp, J. J. *Polym. Sci. Eng.* **1986**, *26*, 418.
(10) Elemans, P. H. M.; Janssen, J. M. H.; Meijer, H. E. H. *J. Rheol.* **1990**, *34***,** 1311.
(11) Cho, K.; Jeon, H. K.; Park, C. E.; Kim, J.; Kim, K. U. *Polymer* **1996**, *37*, 1117.
(12) Luciani, A.; Champagne, M. F.; Utracki, L. A. *J. Polym. Sci., Polym. Phys. Ed.* **1997**, *35*, 1393.
(13) Carriere, C. J.; Cohen, A.; Arends, C. B. *J. Rheol.* **1989**, *33*, 681.
(14) Cohen, A.; Carriere, C. J. *Rheol. Acta* **1989**, *28*, 223.
(15) Carriere, C. J.; Cohen, A. *J. Rheol.* **1991**, *35*, 205.
(16) Rundqvist, T.; Cohen, A.; Klason, C. *Rheol. Acta* **1996**, *35*, 458.
(17) Girault, H. H. J.; Schiffrin, D. J.; Smith, B. D. V. *J. Colloid Interface Sci.* **1984**, *101*, 257.
(18) Watkins, V. H.; Hobbs, S. Y. *Polymer* **1993**, *34*, 3955.
(19) Yoon, P. J.; White, J. L. *J. Appl. Polym. Sci.* **1994**, *51*, 1515.
(20) Luciani, A.; Champagne, M. F.; Utracki, L. A. *Polym. Networks Blends* **1996**, *6*, 51.
(21) Rao, N.; Wanke, S. E.; Sundararaj, U. *Can. Chem. News* **1998**, *4*, 29.
(22) Tomotika, S. *Proc. R. Soc. London* **1935**, *A150*, 322.
(23) Plateau, *Statique expérimentale et Théorique des Liquides Soumis aux seules Forces Moléculaires*, 1873; Vol. 2, p 415.
(24) Rayleigh, L. *Proc. R. Soc. London* **1879**, *29*, 71.
(25) Taylor, G. I. *Proc. R. Soc. London* **1934**, *A146*, 501.
(26) Tjahjadi, M.; Stone, H. A.; Ottino, J. M. *J. Fluid Mech.* **1992**, *243*, 297.
(27) Tjahjadi, M.; Ottino, J. M.; Stone, H. A. *AIChE J.* **1994**, *40*, 385.
(28) Palierne, J. F.; Lequeux, F. *J. Non-Newtonian Fluid Mech.* **1991**, *40*, 289.
(29) Bousmina, M. *Rheol. Acta* **1999**, *38*, 73.
(30) Ellingson, P. C.; Strand, D. A.; Cohen, A.; Sammler, R. L.; Carriere, C. J. *Macromolecules* **1994**, *27*, 1643.
(31) Pham, H. T.; Carriere, C. J. *Polym. Eng. Sci.* **1997**, *37*, 636.
(32) Carriere, C. J.; Silvis, H. C. *J. Appl. Polym. Sci.* **1997**, *66*, 1175.
(33) Kirjava, J.; Rundqvist, T.; Holsti-Miettinen, R.; Heino, M.; Vainio, T. *J. Appl. Polym. Sci.* **1995**, *55*, 1069.
(34) Moussaif, N.; Jerome, R. *Macromol. Symp.* **1999**, *31*, 554.
(35) Rallison, J. M. *Annu. Rev. Fluid Mech.* **1984**, *16*, 45.
(36) Grace, H. P. *Chem. Eng. Commun.* **1982**, *14*, 225.
(37) Kamal, M. R.; Demarquette, N. R.; Lai-Fook, R. A.; Price, T. A. *Polym. Eng. Sci.* **1997**, *37*, 813.
(38) Chen, C. C.; White, J. L. *Polym. Eng. Sci.* **1993**, *33*, 923.
(39) Anastasiadis, S. H.; Gancarz, I.; Koberstein, J. T. *Macromolecules* **1988**, *21*, 2980.
(40) Hu, W.; Koberstein, J. T.; Lingelser, J. P.; Gallot, Y. *Macromolecules* **1995**, *28*, 5209.
(41) Bashforth, F.; Adams, J. C. *An Attempt to Test the Theories of Capillary Action by Comparing the Theoretical and Measured Forms of Drops on Solids*; Cambridge University Press: Cambridge, UK, 1883.
(42) Fox, T. G., Jr.; Flory, P. J. *J. Appl. Phys.* **1950**, *21*, 581.
(43) Garmabi, H. Ph.D. Dissertation, McGill University, 1997.
(44) Wu, S. *J. Macromol. Sci., Rev. Macromol. Chem.* **1974**, *C10*, 1.
(45) Hayami, Y. *Colloid Polym. Sci.* **1996**, *274*, 643.
(46) Scholz, P.; Froelich, D.; Muller, R. *J. Rheol.* **1989**, *33*, 481.
(47) Palierne, J. F. *Rheol. Acta* **1990**, *29*, 204. Erratum **1991**, *30*, 497.
(48) Bousmina, M.; Bataille, P.; Sapieha, S.; Schreiber, H. P. *J. Rheol.* **1995**, *39*, 499.
(49) Friedrich, C.; Gleinser, W.; Korat, E.; Maieer, D.; Weese, J. *J. Rheol.* **1995**, *39*, 1411.
(50) Lacroix, C.; Bousmina, M.; Carreau, P. J.; Favis, B. D.; Michel, A. *Polymer* **1996**, *37*, 2939.
(51) Lacroix, C.; Aressy, M.; Carreau, P. J. *Rheol. Acta* **1997**, *36*, 416.
(52) Hussein, I. A.; Williams, M. C. *Polyblends'99 Symposium*, 217, Oct 13−15, 1999, Boucherville, QC, Canada.

MA000537X